

Received: 2020.03.18

Accepted: 2020.05.22

Available online: 2020.08.18

Published: 2020.10.06

miR-188-3p Inhibits Vascular Smooth Muscle Cell Proliferation and Migration by Targeting Fibroblast Growth Factor 1 (*FGF1*)

Authors' Contribution:

Study Design A

Data Collection B

Statistical Analysis C

Data Interpretation D

Manuscript Preparation E

Literature Search F

Funds Collection G

ACDEG 1 **Shaohua Mi***

ABCE 2 **Pengfei Wang***

AE 3 **Lejun Lin**

1 Department of Cardiology, Yantai Yuhuangding Hospital, Qingdao University, Yantai, Shandong, P.R. China

2 Department of Cardiology, Yantai Yuhuangding Hospital, Laishan Branch, Yantai, Shandong, P.R. China

3 Nuclear Medicine Department, Yantai Yuhuangding Hospital, Qingdao University, Yantai, Shandong, P.R. China

* Shaohua Mi and Pengfei Wang contributed equally

Corresponding Author: Lejun Lin, e-mail: jipanyi08@163.com

Source of support: Departmental sources

Background: As one of the crucial causes leading to cardiovascular disease, atherosclerosis (AS) develops in association with the dysfunction of vascular smooth muscle cells (VSMCs). However, the associated mechanism of the proliferation and migration in VSMCs requires further elucidation.

Material/Methods: Human VSMCs and ApoE-knockout (ApoE^{-/-}) mice were used to establish AS cell and animal models, respectively. Expression levels of miR-188-3p and fibroblast growth factor 1 (*FGF1*) mRNA were detected using quantitative reverse transcription-polymerase chain reaction (qRT-PCR). Western blot was used to assess FGF1 protein expression. The proliferation, migration, and apoptosis of the cells were determined using MTT, BrdU, and Transwell assays, as well as flow cytometry analysis. The interaction between miR-188-3p and *FGF1* was validated using dual-luciferase reporter gene assay, qRT-PCR, and Western blot analysis.

Results: MiR-188-3p was found to be significantly decreased in the serum of AS patients and ApoE^{-/-} mice as well as VSMCs of ApoE^{-/-} mice and human VSMCs treated with oxidized low-density lipoprotein. MiR-188-3p repressed the proliferation and migration of VSMCs but promoted apoptosis of VSMCs. The binding site between miR-188-3p and 3' untranslated region (3'-UTR) of *FGF1* was identified, and *FGF1* was verified as a target gene of miR-188-3p. Restoration of FGF1 reversed the effects of miR-188-3p on VSMCs.

Conclusions: MiR-188-3p suppresses the proliferation and migration of VSMCs and induces their apoptosis through targeting *FGF1*.

MeSH Keywords: **Abdominal Muscles • Dementia, Vascular • Fibroblast Growth Factor 2**

Full-text PDF: <https://www.medscimonit.com/abstract/index/idArt/924394>



3459



1



5



24



Background

Cardiovascular disease (CVD) is recognized as a common cause of death worldwide, with coronary artery disease induced by atherosclerosis (AS) accounting for 45.1% of deaths [1]. During the past decade, the number of deaths caused by AS have increased by 117.2% in East Asia [2]. At present, early diagnosis of AS is still difficult to achieve [1,3,4]. Therefore, it is critical to further explore the molecular mechanisms of AS development to obtain clues for the diagnosis and treatment of AS.

Vascular smooth muscle cells (VSMCs) located in the arterial medial are essential cells in maintaining the integrity of the arterial wall and exhibit critical effects at all stages of AS development [5]. In the early stage of AS, factors such as the release of inflammatory factors elicited by intimal layer damage can induce VSMCs to transform from a contractile phenotype to a synthetic phenotype, migrate to the intima, and then undergo aberrant proliferation to form AS plaques; in the late stage of AS, the apoptosis of VSMCs can trigger the instability of AS plaques [6,7].

Known as small noncoding RNAs, microRNAs (miRNAs) are approximately 22 nucleotides in length. An increasing number of studies have elucidated that miRNAs exert a regulatory effect on the development of AS. For instance, in oxidized low-density lipoprotein (ox-LDL)-stimulated macrophages, miR-497 promotes the accumulation of lipids, which suggests the potential to promote AS [8]. MiR-188-3p has been reported to have critical functions in cancer progression, myocardial infarction, and other diseases in recent years. In cancer biology, miR-188-3p often acts as a tumor suppressor [9,10]. For example, in pancreatic cancer, miR-188-3p represses the colony-forming ability of cancer cells by specific inhibition of BRD4 [9]. In addition, after miR-188-3p mimics were injected into ApoE-knockout (ApoE^{-/-}) mice, the lipid accumulation, macrophage recruitment, and levels of inflammatory factors in the aorta of the mice were significantly ameliorated [11]. This outcome suggests that miR-188-3p has potential inhibitory effects on the development of AS. However, whether miR-188-3p can attenuate the dysfunction of VSMCs is still unknown.

Fibroblast growth factor 1 (FGF1) serves as an important inflammatory factor in a majority of CVDs, such as myocardial ischemia-reperfusion injury, hypertension, and myocardial infarction [12–14]. FGF1 also plays a role in the development of AS. For example, in mouse VSMCs and monocytes, overexpression of FGF1 can bolster inflammatory responses and the proliferation of cells [13]. In human VSMCs treated with ox-LDL, FGF1 expression is abnormally increased, and overexpression of FGF1 significantly accelerates the proliferation and migration of VSMCs [15].

In our study, we used bioinformatics analysis and found that miR-188-3p was aberrantly expressed in multiple AS-related miRNA expression profile datasets. We also noted a potential binding site between miR-88-3p and the 3' untranslated region (3'-UTR) of *FGF1*. Therefore, we hypothesized that the miR-188-3p/FGF1 axis plays a role in the development of AS by regulating the phenotypes of VSMCs. This study evaluated the role of miR-188-3p/FGF1 in VSMCs and offers a theoretical foundation for the molecular mechanism in AS development.

Material and Methods

Bioinformatics analysis

In GSE34647, female ApoE^{-/-} mice were fed a high-fat diet for 3 or 10 months. Afterward, expression of miRNAs in AS plaque was measured. In the GSE89858 dataset, double-knockout Apobtm2Sgy/Ldltm1Her mice had been fed with either high-fat or normal chow diet. Mice were euthanized after 0, 6, 18, and 30 weeks, and expression of miRNAs in ascending aortas with AS lesions was measured. After matrix dataset downloading, miRNAs with *P* value <0.05 and $|\log_2FC| >1.5$ were selected for heatmap building. All miRNAs were selected to build volcano plot.

Clinical samples

Fifty-four patients who underwent coronary angiography between March 2016 and July 2017 were randomly enrolled in this study. All patients had $\geq 50\%$ arteriostenosis of no less than one main coronary artery. None of the patients had valvular heart disease, liver disease, renal failure, autoimmune diseases, or other inflammatory diseases. Serum samples from these patients were collected. For the control group, serum samples were also collected from 54 healthy volunteers who had undergone health examinations in Yantai Yuhuangding Hospital. The serum samples were stored at -80°C immediately after collection. All subjects gave informed written consent. This study was approved by the Research Ethics Committee of Yuhuangding Hospital.

Cell culture and transfection

Human VSMCs were obtained from the Cell Center of the Chinese Academy of Medical Sciences (Shanghai, China), cultured in Dulbecco's modified Eagle's medium (DMEM; HyClone, Logan, UT, USA) supplemented with 10% fetal bovine serum (FBS, HyClone), 100 U/mL penicillin, and 100 $\mu\text{g}/\text{mL}$ streptomycin (Sigma, St. Louis, MO, USA) at 37°C in 5% CO_2 . The cells in the logarithmic growth phase were used for follow-up experiments.

Table 1. Primer sequences used for PCR.

Name	Primer sequences
MiR-188-3p	Forward: 5'-ATTATTGGCTCCACATGCAG-3'
	Reverse: 5'-ATCCAGTGCAGGGTCCGAGG-3'
U6	Forward: 5'-CTCGCTTCGGCAGCAC-3'
	Reverse: 5'-AACGCTTCACGAATTTGCGT-3'
FGF1	Forward: 5'-AATGGGAGCTGCAAACGCGTCC-3'
	Reverse: 5'-TCAACAGGTGAGGACCCCTCGA-3'
GAPDH	Forward: 5'-CCAGGTGGTCTCTCTGA-3'
	Reverse: 5'-GCTGTAGCCAAATCGTTGT-3'

We purchased pcDNA3.1-control, pcDNA3.1-FGF1, miRNA mimics control (mimics-NC), miRNA inhibitors control (inhibitors-NC), miR-188-3p mimics, and miR-188-3p inhibitors from GenePharma Co., Ltd. (Shanghai, China). VSMCs were harvested and seeded into a 24-well plate at a density of 3×10^5 cells/well, and cell transfection was performed after 24 h of culture. VSMCs were transfected using Lipofectamine 3000 (Invitrogen, Carlsbad, CA, USA) conforming to the protocols.

Establishment of *in vitro* AS cell model

VSMCs were treated with 0, 25, 50, and 100 mg/L ox-LDL for 24 or 48 h to establish *in vitro* AS cell models for subsequent experiments.

Animal models

The animal experimental protocol was approved by the Animal Ethics Committee of Yuhuangding Hospital. Eight-week-old C56BL/6J mice were available from the Animal Center of Qilu Hospital (Jinan, China). Five mice were ApoE^{-/-} mice, which were fed high-fat diets to establish the AS models, and 5 mice were wild-type (WT) mice, which were fed normal diets. All mice were maintained at room temperature (18–22°C) at a relative humidity of 50–60%.

Quantitative reverse transcription–polymerase chain reaction (qRT-PCR)

Total RNAs were extracted from serum samples using serum microRNA rapid extraction kit (Bioteke, Beijing, China) and total RNAs in VSMCs were extracted using TRIzol reagent (Invitrogen). The concentration and purity of the extracted RNAs were measured using Thermo NanoDrop 2000. All primers in the study shown in Table 1 were designed and synthesized by TaKaRa (Dalian, China). The extracted RNA was reverse-transcribed into cDNAs with Reverse Transcription Kit (Takara). PCR amplification was performed according to the instructions of SYBR Premix Ex Taq™ II (Takara). The relative

expression of miR-188-3p and *FGF1* mRNA was calculated using $2^{-\Delta\Delta CT}$ method.

Western blot analysis

Total protein was extracted from VSMCs using RIPA lysis buffer (Beyotime Biotechnology, Shanghai, China), and the concentration of the extracted protein was detected using the Bradford method. After being denatured, the protein samples were subjected to SDS-PAGE. Subsequently, the protein in the gel was transferred to nitrocellulose membranes (Millipore, Bedford, MA, USA). After being blocked with 5% skimmed milk at room temperature for 1 h, the membranes were incubated with primary anti-FGF1 polyclonal antibody (Abcam, Shanghai, China, ab9588, diluted 1: 500) overnight at 4°C. Following that, the membranes were washed using TBST for 20 min and then incubated with secondary antibody (Abcam, ab205718, diluted 1: 3000) for 1 h at room temperature. After membranes were again rinsed with TBST, the protein bands were visualized and imaged using ECL chemiluminescence solution (Amersham Pharmacia Biotech, Little Chalfont, UK).

MTT assay

VSMCs in the logarithmic growth phase were harvested. The cell density of the obtained cell suspension was modulated to 4×10^4 /mL using complete medium, and then 100 μ L of the cell suspension was added to each well on a 96-well culture plate. After 24 h of culture, most cells adhered to the bottom of the wells, and the original medium was replaced with medium supplemented with 0.5% FBS. Twenty-four hours later, the above medium was removed, and 10 μ L of 5 mg/mL MTT solution (Beyotime Biotechnology) was added to each well. Notably, 6 replicate wells were used for each group. After 4 h of incubation at 37°C in 5% CO₂, the solution of each well was discarded, 150 μ L of dimethyl sulfoxide (Beyotime Biotechnology) was added to each well, and the incubation was maintained for another 10 min on a shaker. After the precipitate was completely dissolved, the optical density value was measured at a wavelength of 490 nm using a microplate reader.

BrdU assay

VSMCs in the logarithmic growth phase were harvested to make single-cell suspensions, and 1×10^5 cells/well were seeded into 24-well plates. After the cells adhered to the bottom of the wells, BrdU labeling reagent (Wuhan AmyJet Scientific Inc., Wuhan, China) was added to each well according to instructions, and the plates were maintained in 5% CO₂ at 37°C. After 8 h of culture, the medium was discarded, and the cells were fixed with 4% paraformaldehyde. Then 2 mol/L HCl was added to denature the DNA of the cells. The cells were then washed with PBS, and anti-BrdU antibody (Beyotime Biotechnology)

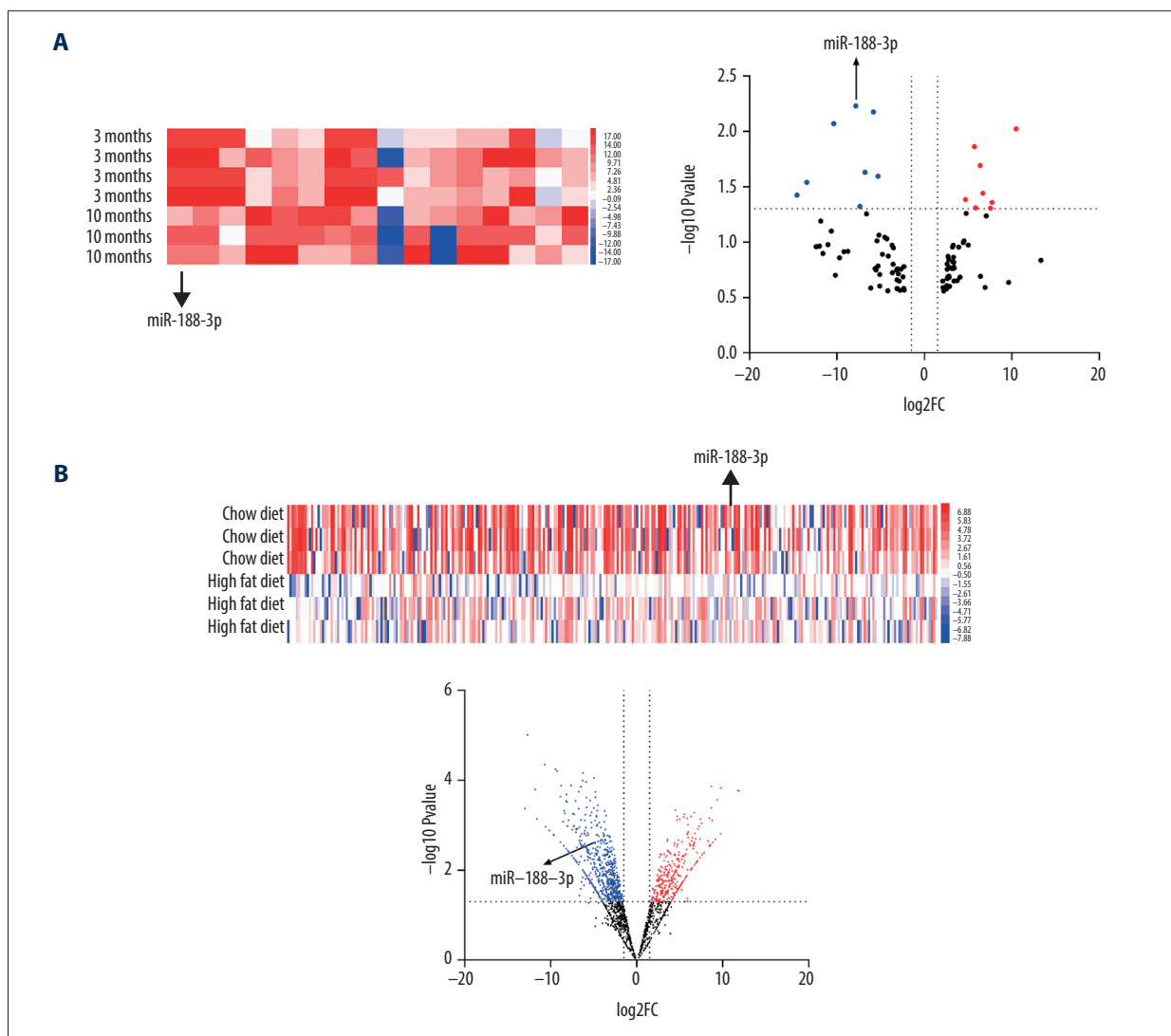


Figure 1. Expression of miR-188-3p in the Gene Chip dataset. **(A, B)** miR-188-3p was found to be significantly decreased in AS plaques derived from mice fed a high-fat diet for 10 months compared with mice fed a high-fat diet for 3 months based on the dataset GSE34647. **(C, D)** miR-188-3p was found to be significantly reduced in the ascending aorta of mice fed a high-fat diet based on the dataset GSE89858.

was added prior to incubation of the cells at 4°C for 12 h. Next, DAPI solution (Beyotime Biotechnology) was added to stain the nuclei for 30 min. Under the fluorescence microscope, 3 fields were randomly selected and the number of the cells in each field was counted. The cell proliferation was calculated as follows: cell proliferation rate=number of BrdU-positive cells/number of DAPI-positive cells. The mean value of the cell proliferation rates in 3 fields was adopted as the proliferation rate for the cells in each group.

Transwell assay

Twenty-four hours after transfection, the cells in each group were trypsinized, and resuspended using serum-free DMEM to

modulate the cell concentration to 1×10⁵ cells/mL. Subsequently, 200 μL of cell suspension was added to the upper chamber of the Transwell system (8 μm, Corning, Beijing, China), and 500 μL of DMEM containing 10% FBS was added to the bottom chamber. The culture was sustained at 37°C in 5% CO₂ for 48 h. Subsequently, the upper chamber was removed and the cells that had migrated to the bottom were processed as follows: fixed using 4% paraformaldehyde for 15 min, stained using 0.1% crystal violet solution for 15 min, and washed with PBS to remove residual crystal violet. Additionally, the cells that failed to pass through the membrane were carefully wiped off using a cotton swab. Ultimately, the cells were observed under a microscope, 5 fields were randomly selected, the number of migrating cells in each field was counted, and the average number was calculated.

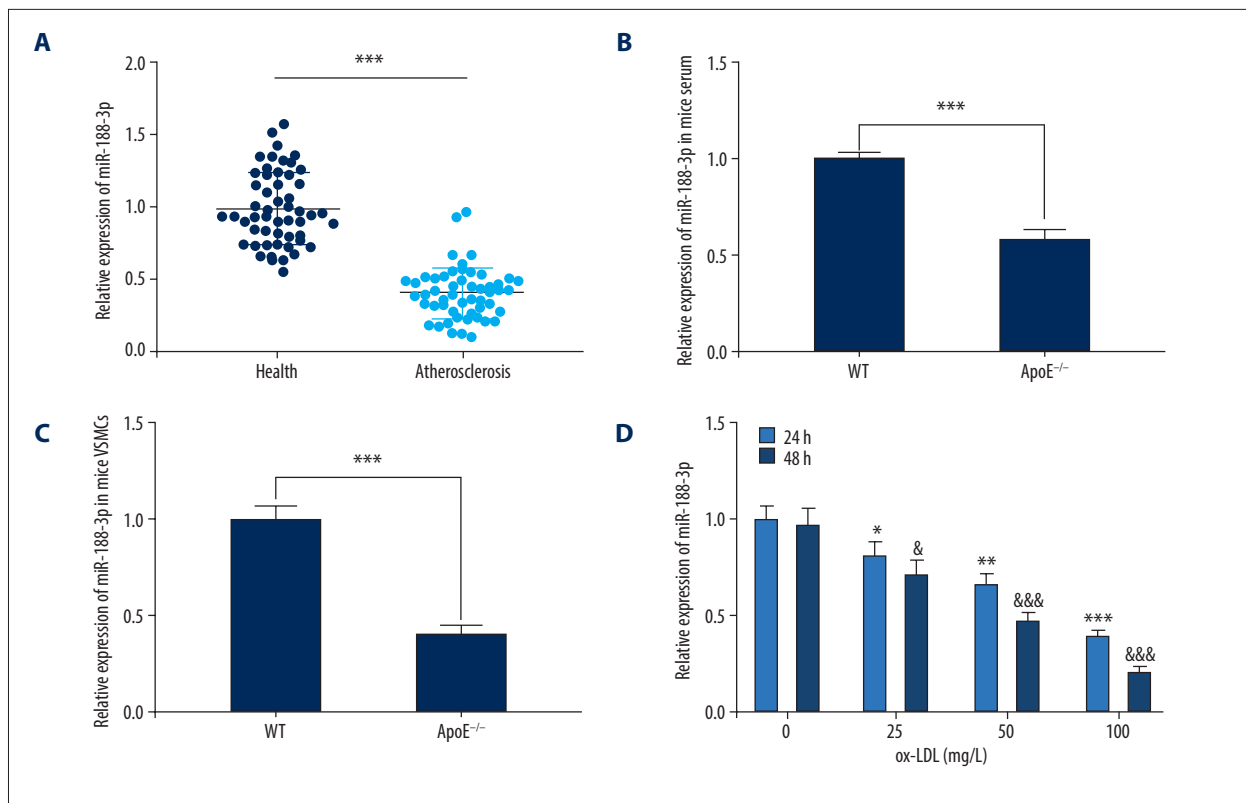


Figure 2. Expression of miR-188-3p in AS patients, mice, and ox-LDL-treated VSMCs. **(A)** Expression level of miR-188-3p in serum of AS patients and healthy controls. **(B, C)** miR-188-3p expression in mouse serum and carotid smooth muscle cells. **(D)** Expression of miR-188-3p in ox-LDL-treated VSMCs. * $P < 0.001$. In **D**, * $P < 0.05$, ** $P < 0.01$, and *** $P < 0.001$, compared with the 0 mg/L group after 24 h of ox-LDL treatment; & $P < 0.05$, and &&& $P < 0.001$, compared with the 0 mg/L group after 48 h of ox-LDL treatment.

Apoptosis assay

After the cells were treated with different factors, the cells were trypsinized and harvested using centrifugation (1500 rpm, 3 min). Cell apoptosis was detected using the Apoptosis Detection Kit (Yeasen Biotech Co., Ltd., Shanghai, China) as follows: after 2×10^5 cells were washed twice using PBS, 100 μ L of binding buffer was added, followed by 10 μ L of AnnexinV-FITC solution and 5 μ L of PI solution, respectively. After incubation at 4°C in the dark for 30 min, the prepared cells were immediately subjected to flow cytometry, and the percentage of apoptotic cells was calculated after the associated data were processed using software.

Dual-luciferase reporter gene assay

The specific binding relationship between miR-188-3p and the 3'-UTR of *FGF1* was validated using dual-luciferase reporter gene assay. The reporter gene vector pmirGLO-*FGF1*-WT was constructed with *FGF1* WT 3'-UTR fragment, which contained the binding site, and was cloned into the pmirGLO dual-luciferase gene vector (Promega Corp., Madison, WI, USA). GeneArt

Site-Directed Mutagenesis PLUS System (cat. No. A14604; Thermo Fisher Scientific, Inc., Waltham, MA, USA) was used to mutate the putative binding site of *FGF1*. The mutant (MUT) *FGF1* 3'-UTR fragment was cloned into the pmirGLO vector to establish the pmirGLO-*FGF1*-MUT. pmirGLO-*FGF1*-WT or pmirGLO-*FGF1*-MUT and miR-188-3p mimics or mimics-NC were co-transfected into VSMCs, respectively, using Lipofectamine 3000 (Invitrogen), and subsequently, the cells were cultured for another 48 h. Following that, luciferase activity of each group was detected using the Dual-Luciferase Reporter Assay System (Promega, Madison, WI, USA).

Statistical analysis

SPSS 22.0 statistical software (SPSS Inc., Chicago, IL, USA) was used for statistical analysis. Measurement data were expressed as mean \pm variance ($\bar{x} \pm s$). Independent sample *t*-test and rank test were used to compare the difference between every 2 groups. Statistical differences were considered significant at $P < 0.05$.

Results

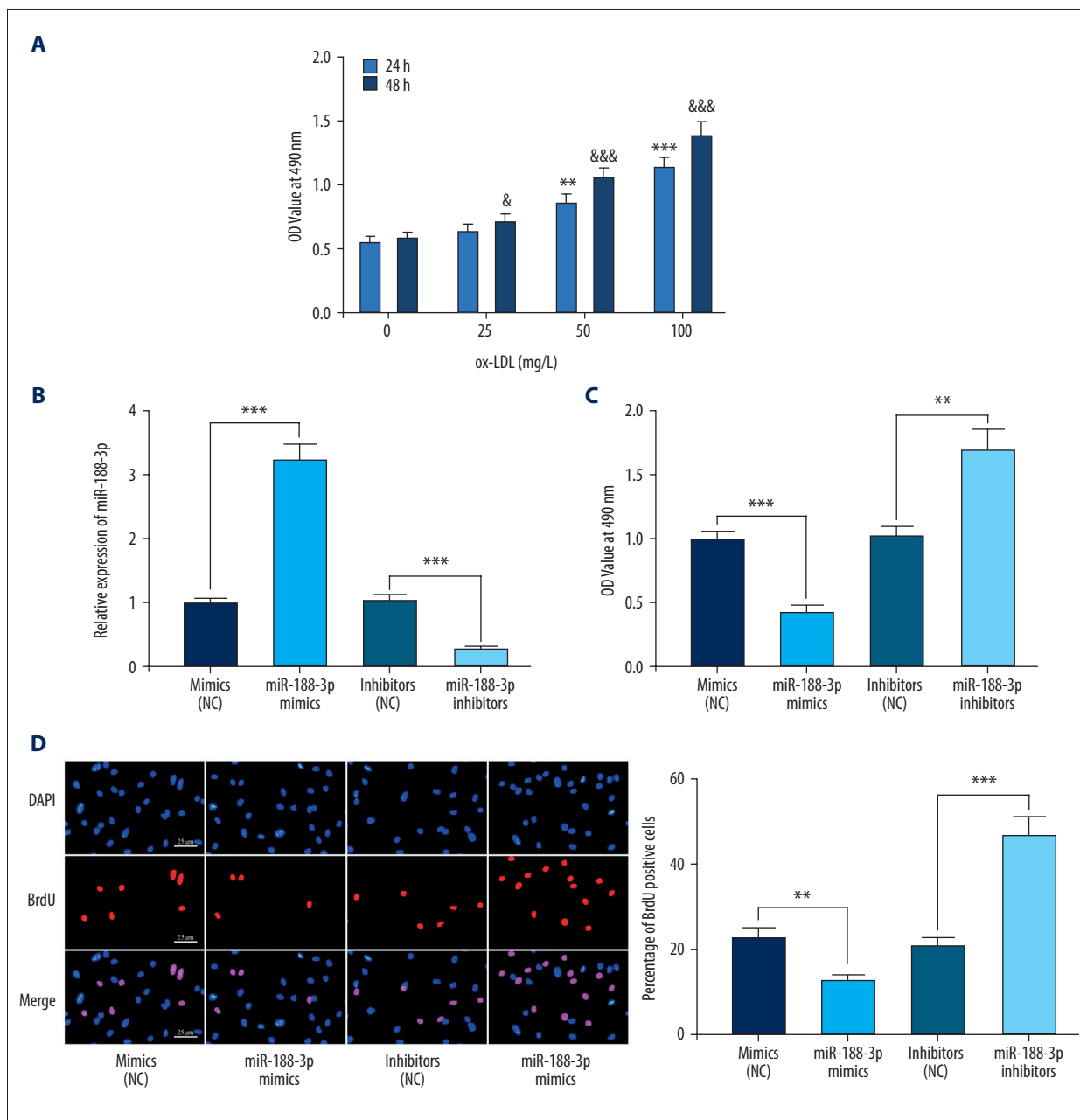
Discovery of miR-188-3p

Based on the public microarray database GSE34647, miR-188-3p expression level was observed to be remarkably reduced in AS plaques derived from mice fed a high-fat diets for 10 months compared with mice fed a high-fat diet for 3 months after the AS model was established using ApoE^{-/-} mice (Figure 1A, 1B). In GSE89858, similarly, it was found that in an animal model of AS established by Apobtm2Sgy/Ldltm1Her double-knock-out mice, the miR-188-3p expression level was remarkably

reduced in the ascending aorta of mice fed a high-fat diets for 30 weeks compared with mice fed a normal diet for 30 weeks (Figure 1C, 1D). Therefore, we speculated that the dysregulation of miR-188-3p may play a role in AS progression.

Abnormal expression of miR-188-3p during AS development

To detect miR-188-3p expression during AS development, we examined its expression level using qRT-PCR. miR-188-3p expression was observed to be markedly reduced in serum derived from AS patients compared with healthy volunteers (Figure 2A).



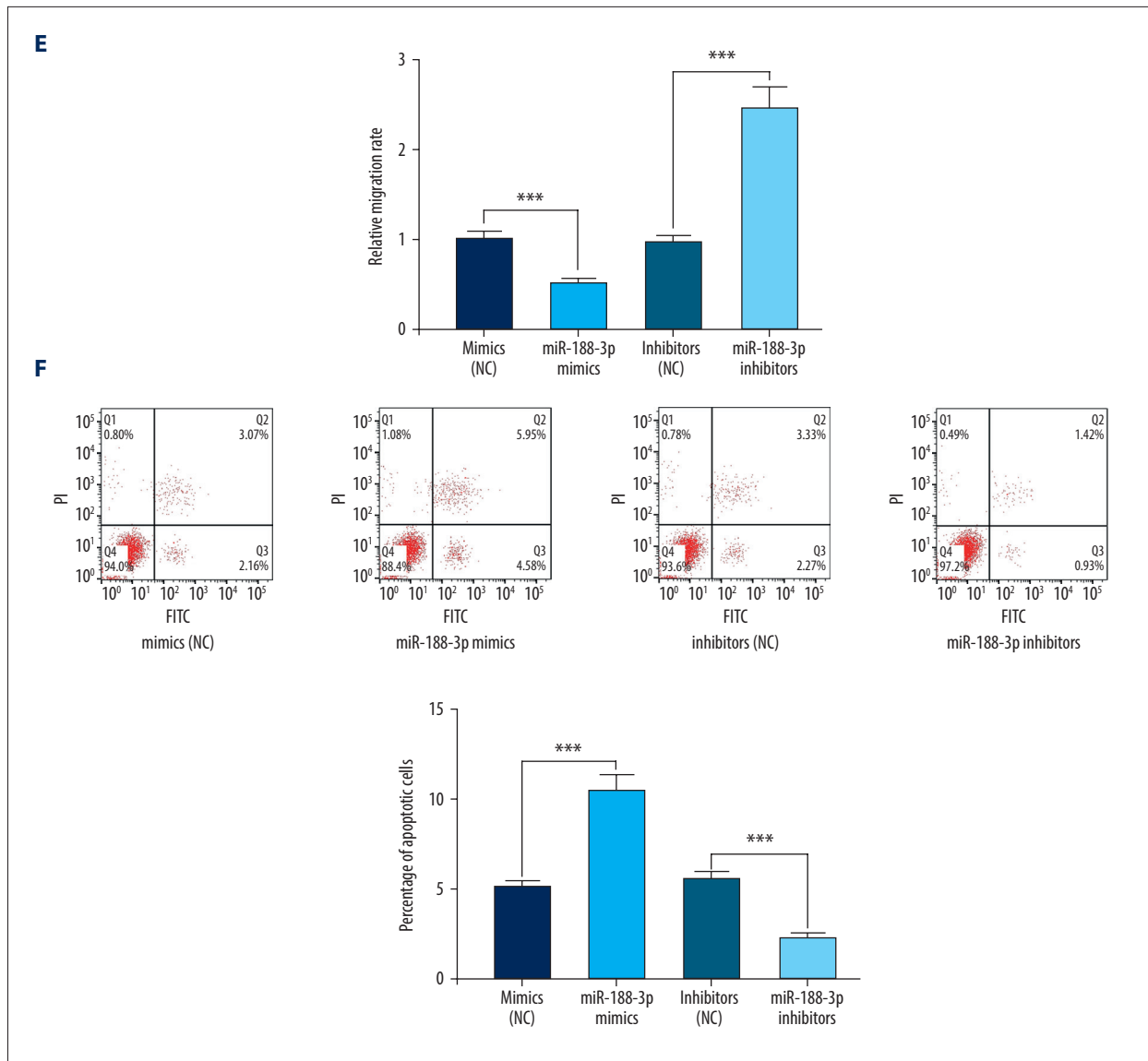
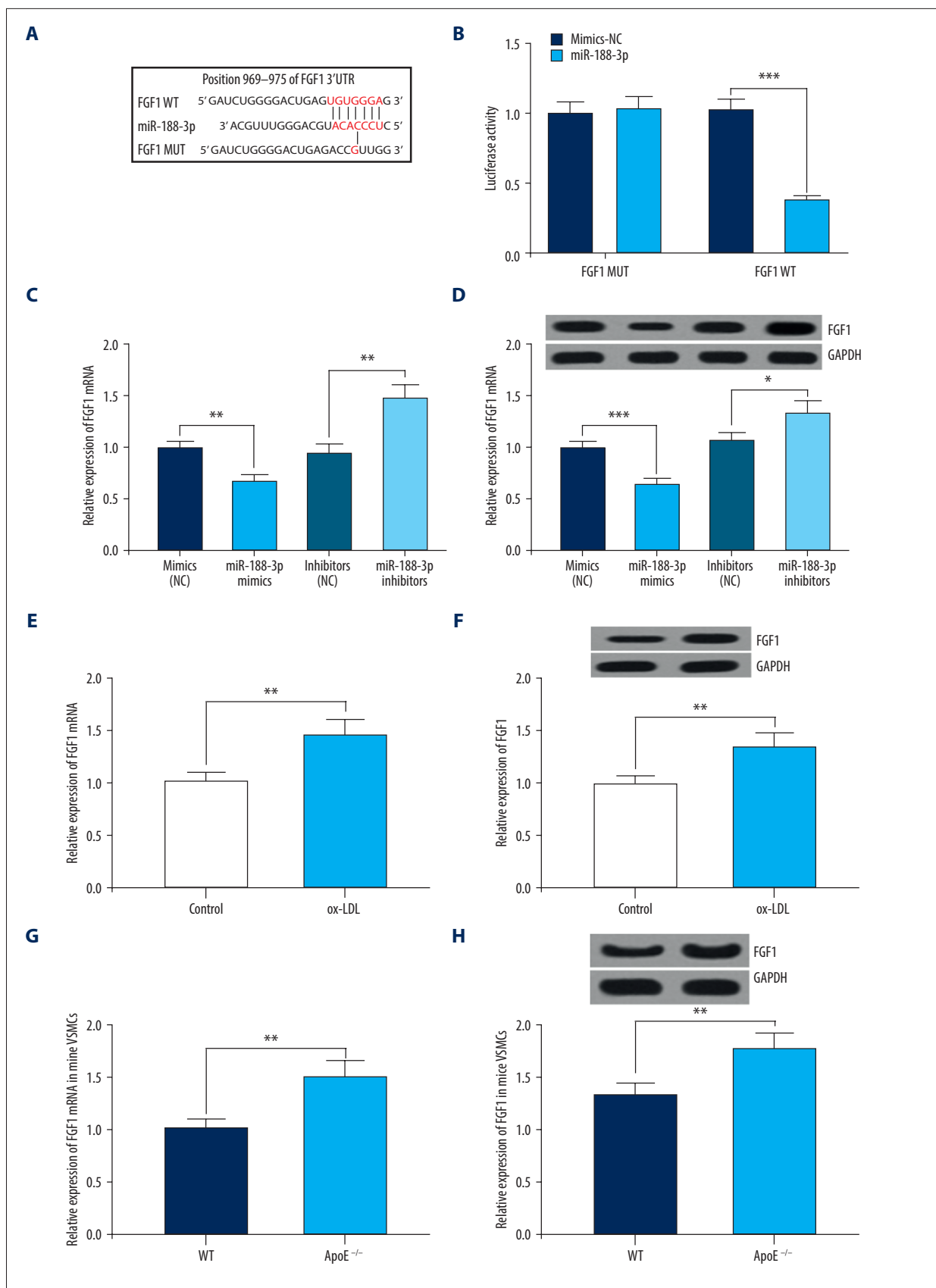


Figure 3. Effect of miR-188-3p on VSMCs. (A) The effects of ox-LDL with different treatment durations and concentrations on the viability of VSMCs were detected using the MTT assay. (B) The establishment of miR-188-3p overexpression and low-expression cell models was validated using qRT-PCR. (C) The effect of miR-188-3p on VSMCs proliferation was examined using the BrdU assay. (D) The effect of miR-188-3p on the migration of VSMCs was examined using the Transwell assay. (E) The effect of miR-188-3p on the migration of VSMCs was examined using the Transwell assay. (F) The effect of miR-188-3p on apoptosis of VSMCs was examined using flow cytometry. ** $P < 0.01$, and *** $P < 0.001$. In A, ** $P < 0.01$, and *** $P < 0.001$, compared with the 0 mg/L group after 24 h of ox-LDL treatment; & $P < 0.05$, and && $P < 0.001$, respectively, compared with the 0 mg/L group after 48 h of ox-LDL treatment.

In serum and carotid smooth muscle cells derived from mouse models of AS, we observed similar results (Figure 2B, 2C). We further found that ox-LDL markedly downregulated miR-188-3p expression in ox-LDL-treated VSMCs, which showed time-dependent and concentration-dependent effects (Figure 2D). All of these data supported that miR-188-3p was abnormally downregulated during AS development.

miR-188-3p affected the proliferation, migration, and apoptosis of VSMCs

The effect of ox-LDL was assessed on the proliferation of VSMCs at different concentrations and treatment durations using MTT. We noted that the viability of VSMCs was the highest at 100 mg/L for 48 h (Figure 3A), and the miR-188-3p expression levels were the lowest under the same condition (Figure 2D).



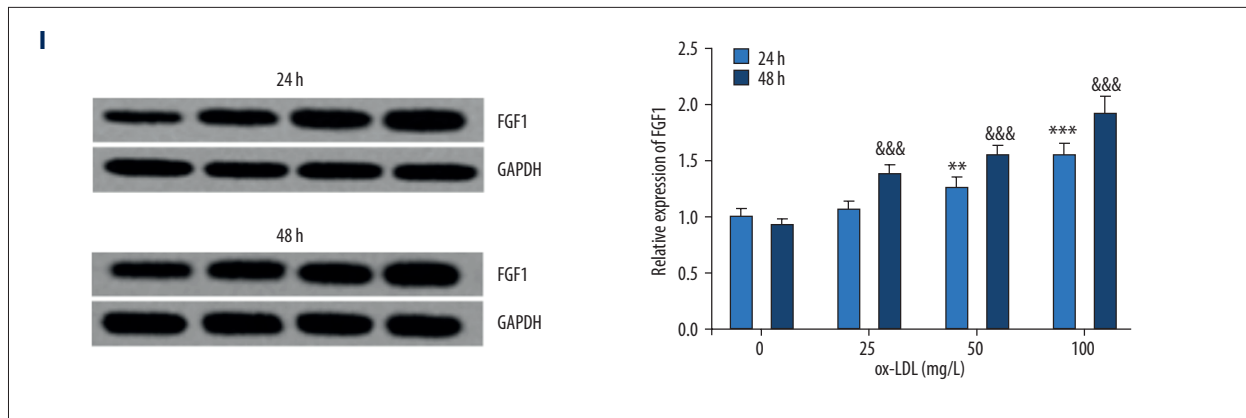


Figure 4. Interaction between miR-188-3p and *FGF1*. (A) Binding site between miR-188-3p and the 3'UTR of *FGF1* was predicted using TargetScan database. (B) Binding site between miR-188-3p and the 3'UTR of *FGF1* was verified using dual-luciferase reporter gene assay. (C) The effect of miR-188-3p on *FGF1* expression was examined using qRT-PCR. (D) The effect of miR-188-3p on *FGF1* mRNA expression was examined using Western blot analysis. (E) The effect of ox-LDL treatment on *FGF1* mRNA expression in VSMCs was examined using qRT-PCR. (F) The effect of ox-LDL treatment on *FGF1* expression levels in VSMCs was examined by Western blot analysis. (G) *FGF1* mRNA expression in carotid smooth muscle cells from WT and AS mice was measured using qRT-PCR. (H) *FGF1* expression in carotid smooth muscle cells from WT and AS mice was measured using qRT-PCR. (I) Expression of *FGF1* in ox-LDL-treated VSMCs. * $P < 0.05$, ** $P < 0.01$, and *** $P < 0.001$. In I, * $P < 0.01$, and *** $P < 0.001$, compared with the 0 mg/L group after 24 h of ox-LDL treatment; &&& $P < 0.001$, compared with the 0 mg/L group after 48 h of ox-LDL treatment.

Therefore, we used 100 mg/L ox-LDL to treat VSMCs for 48 h to perform the following experiments. We transfected miR-188-3p mimics and inhibitors into VSMCs to establish cell models of miR-188-3p overexpression and low expression, respectively (Figure 3B). The results of the MTT and BrdU assays supported that miR-188-3p overexpression markedly minimized the viability of VSMCs, while the opposite result was observed when the expression of miR-188-3p was inhibited (Figure 3C, 3D). In the Transwell assay, the migration of cells in the miR-188-3p mimics group was markedly suppressed compared with the control group, and the transfection of miR-188-3p inhibitors significantly promoted the migration of VSMCs (Figure 3E). The results of flow cytometry analysis further suggested that miR-188-3p had a role in promoting apoptosis of VSMCs (Figure 3F). Our results indicated that miR-188-3p alleviated the dysfunction of VSMCs.

FGF1 was specifically regulated by miR-188-3p

To explore how miR-188-3p exerted its effects in VSMCs, the downstream target genes of miR-188-3p were predicted using TargetScan, miRWalk, and miRmap, and we found that *FGF1*, which is closely related to the proliferation and migration of VSMCs [14], was one of the downstream target genes of miR-188-3p (Figure 4A). Through dual-luciferase reporter gene assay, miR-188-3p mimics were observed to remarkably inhibit the luciferase activity of the pmirGLO-*FGF1*-WT group, but no substantial change was noted in the pmirGLO-*FGF1*-MUT group (Figure 4B). The results of qRT-PCR and Western blot analysis suggested that miR-188-3p remarkably downregulated

the expression of *FGF1* at both the mRNA and protein levels (Figure 4C, 4D). In addition, we detected the expression of *FGF1* at both the mRNA and protein levels in ox-LDL-treated VSMCs and found that *FGF1* expression was remarkably increased compared with control group, in contrast to changes in miR-188-3p expression (Figure 4E–4G). Additionally, compared with the control group, the expression of *FGF1* in VSMCs derived from ApoE^{-/-} mice fed a high-fat diet was also significantly inhibited (Figure 4E–4H). In addition, *FGF1* expression in VSMCs induced by ox-LDL was significantly increased in a dose-dependent and time-dependent manner, which was contrary to miR-188-3p (Figure 4I). The above results confirmed that miR-188-3p could specifically inhibit *FGF1* expression.

FGF1 enhanced the dysfunction of VSMCs

Next, we co-transfected miR-188-3p and pcDNA3.1-*FGF1* into ox-LDL-treated VSMCs and found that *FGF1* supplementation showed no obvious effect on the expression of miR-188-3p, but interfered with the expression of *FGF1* at both the mRNA and protein levels (Figure 5A–5C), suggesting that the way miR-188-3p regulated the expression of *FGF1* was unidirectional. Based on the functional experiments in VSMCs, *FGF1* overexpression was found to significantly attenuate the inhibitory effects of miR-188-3p on the proliferation of VSMCs, and the migration of VSMCs was also remarkably improved (Figure 5D–5F). Further, it was confirmed with flow cytometry that the apoptosis rate of the cells in miR-188-3p mimics+pcDNA3.1-*FGF1* group was obviously lower than that of the miR-188-3p mimics group (Figure 5G). The above results demonstrate that *FGF1*

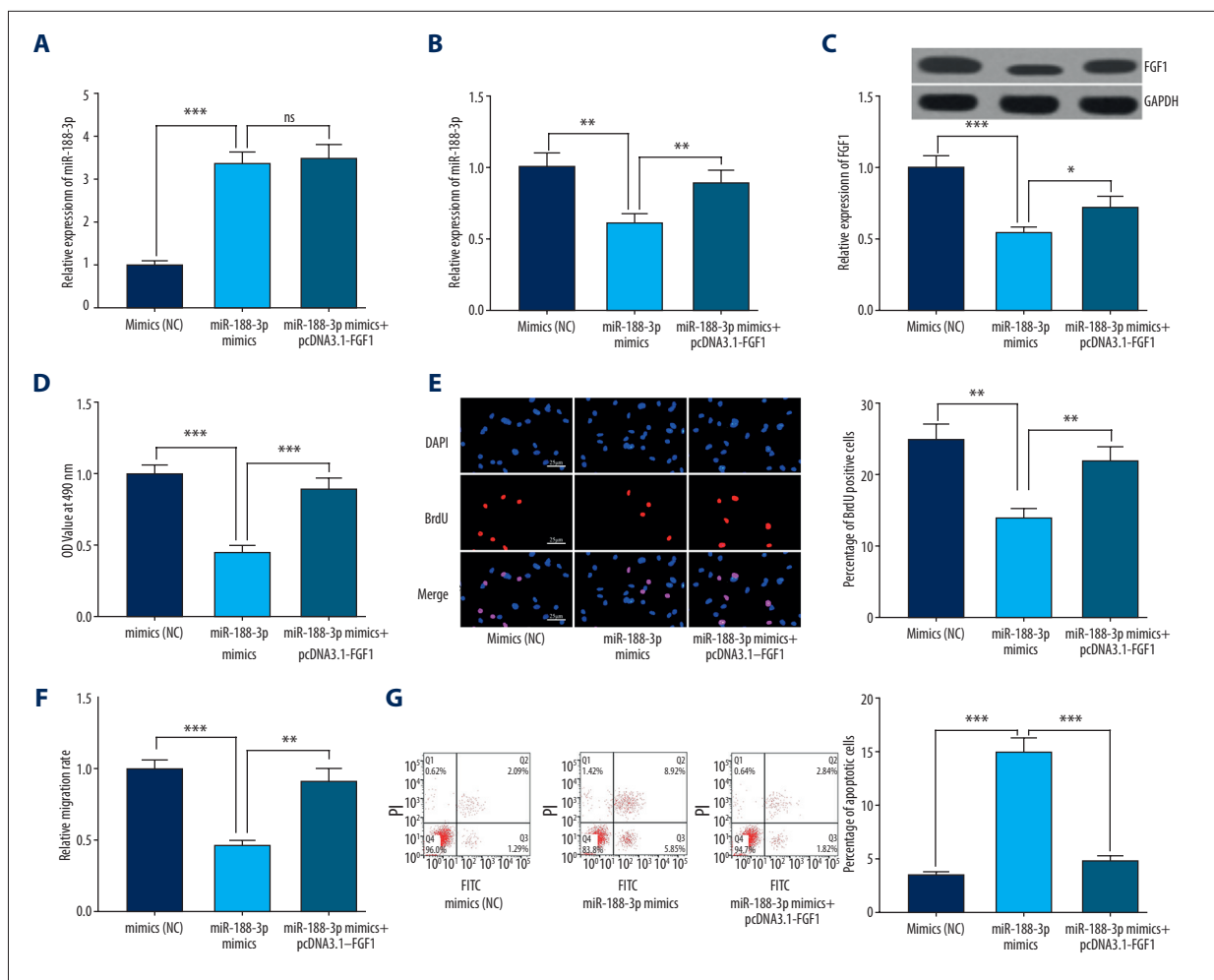


Figure 5. The reversal effect of FGF1 on miR-188-3p function. (A) The effect of co-transfection of miR-188-3p and pcDNA3.1-FGF1 on miR-188-3p expression was examined using qRT-PCR. (B) The effect of co-transfection of miR-188-3p and pcDNA3.1-FGF1 on FGF1 mRNA expression was examined using qRT-PCR. (C) The effect of co-transfection of miR-188-3p and pcDNA3.1-FGF1 on FGF1 expression was examined using Western blot analysis. (D) The proliferation of VSMCs was examined using the MTT assay. (E) The proliferation of VSMCs was examined using the BrdU assay. (F) The migration of VSMCs was examined by the Transwell assay. (G) The apoptosis of VSMCs was examined using flow cytometry. * $P < 0.05$, ** $P < 0.01$, and *** $P < 0.001$.

overexpression inhibited the effect of miR-188-3p, and they further validate that regulatory relationship existed between miR-188-3p and *FGF1*.

Discussion

Increasingly, miRNAs have been found to affect AS progression. For example, in ox-LDL-stimulated human aortic smooth muscle cells, miR-647 expression is significantly increased, and miR-647 promotes cell proliferation and migration by inactivating the PTEN/PI3K/AKT signaling pathway, which accelerates AS progression [16]. In addition, miR-377 expression in serum derived from hypertriglyceridemic patients was significantly lower than that in serum from healthy people, and

miR-377 was found to inhibit the expression of DNA methyltransferase 1, facilitate the binding between lipoprotein lipase and high-density lipoprotein binding protein 1, promote triglyceride hydrolysis, and remarkably reduce AS lesions in animal models [17]. In the current study, we found that miR-188-3p expression levels were markedly downregulated in AS patients, AS mice, and ox-LDL-stimulated VSMCs. Moreover, based on the results of MTT, BrdU, and Transwell assays, as well as flow cytometry analysis, we found that miR-188-3p had inhibitory effects on the proliferation and migration of VSMCs, and promotion effects on apoptosis. MiR-188-3p often plays a cancer-suppressing role in cancer. For example, in breast cancer, miR-188-3p has been confirmed to be abnormally downregulated and to be able to inhibit the proliferation, migration, and invasion of cancer cells through specifically inhibiting

TMED3 [18]. MiR-188-3p expression is significantly upregulated in sevoflurane-induced spatial cognitive impairment, and miR-188-3p can inhibit MDM2 expression, and thus enhance the stability of p53 protein, inducing the apoptosis of neural cells [19]. The role of miR-188-3p in inhibiting proliferation and migration and in promoting apoptosis in the above pathological processes is consistent with the results presented in this study. Furthermore, in previous studies, miR-188-3p has also been found to reduce the inflammatory responses in AS, which also suggests that miR-188-3p is a protective factor in the development of AS [4,11]. Considering previous reports and the results in the present work, we conclude that miR-188-3p is a promising target for the prevention and treatment of AS.

FGF1 expression is significantly increased in atherosclerotic vascular samples compared with normal arterial tissue, and ox-LDL-induced FGF1 release has been confirmed to be one of the factors promoting the proliferation of endothelial cells and VSMCs, which in turn promote AS progression [15,20,21]. In recent years, the upstream mechanism of FGF1 dysregulation in VSMCs has been gradually elucidated. For example, in ox-LDL-treated human aortic smooth muscle cells (HASMCs), the overexpression of lncRNA TNK2-AS1 indirectly upregulates the expression levels of vascular endothelial growth factor A and FGF1 by inhibiting miR-150-5p, and thus enhances the proliferation and migration of HASMCs [22]. In this work, we found the expression of FGF1 in ox-LDL-stimulated VSMCs and carotid smooth muscle derived from ApoE^{-/-} mice fed a high-fat diet was remarkably increased. Based on bioinformatics analysis and the results of dual-luciferase reporter gene assay, we further found that *FGF1* was negatively regulated by miR-188-3p. Additionally, we found that the inhibitory effects of miR-188-3p on the proliferation and migration of VSMCs and its promoting effects on apoptosis were counteracted, which was achieved through the co-transfection of miR-188-3p mimics

and pcDNA3.1-FGF1. Our findings are consistent with the reported role of FGF1 in previous studies and further elucidate its upstream regulatory mechanisms. However, in the development of AS, the downstream regulatory mechanisms of FGF1 are not fully understood. It was previously found that FGF1 and MAPK signaling pathways can be mutually regulated, and both p38 and Erk can inhibit FGF1-induced signaling transduction [23]. In acute kidney injury, it was reported that the mutant of FGF1 can activate GSK-3 β /Nrf2 and ASK1/JNK signaling pathways by activating PI3K/AKT signaling pathway and subsequently exerting anti-inflammatory and antioxidative stress effects [24]. Nonetheless, the mechanism by which FGF1 exerts its effects on the dysfunction of VSMCs still requires further investigation.

Conclusions

In summary, we noted that miR-188-3p expression was abnormally reduced during AS development through *in vitro* and *in vivo* experiments, which exerted inhibitory effects on the proliferation and migration of VSMCs by specifically down-regulating FGF1. Our present research further elucidates the associated molecular mechanism of AS development and provides a theoretical basis for exploring novel targets for prevention and treatment of AS.

Data availability statement

The data used to support the findings of this study are available from the corresponding author upon request.

Conflict of interests

None.

References:

1. Bruikman CS, Stoekenbroek RM, Hovingh GK, Kastelein JP: New drugs for atherosclerosis. *Can J Cardiol*, 2017; 33(3): 350–57
2. Wong MC, Zhang DX, Wang HH: Rapid emergence of atherosclerosis in Asia: a systematic review of coronary atherosclerotic heart disease epidemiology and implications for prevention and control strategies. *Curr Opin Lipidol*, 2015; 26(4): 257–69
3. Bejarano J, Navarro-Marquez M, Morales-Zavala F et al: Nanoparticles for diagnosis and therapy of atherosclerosis and myocardial infarction: Evolution toward prospective theranostic approaches. *Theranostics*. 2018;8(17): 4710–32
4. Verweij SL, van der Valk FM, Stroes ES: Novel directions in inflammation as a therapeutic target in atherosclerosis. *Curr Opin Lipidol*, 2015; 26(6): 580–85
5. Hu D, Yin C, Luo S, Habenicht AJR, Mohanta SK: Vascular smooth muscle cells contribute to atherosclerosis immunity. *Front Immunol*, 2019; 10: 1101
6. Leeper NJ, Maegdefessel L: Non-coding RNAs: Key regulators of smooth muscle cell fate in vascular disease. *Cardiovasc Res*, 2018; 114(4): 611–21
7. Rudijanto A: The role of vascular smooth muscle cells on the pathogenesis of atherosclerosis. *Acta Med Indones*, 2007; 39(2): 86–93
8. Cui J, Ren Z, Zou W, Jiang Y: miR-497 accelerates oxidized low-density lipoprotein-induced lipid accumulation in macrophages by repressing the expression of apelin. *Cell Biol Int*, 2017; 41(9): 1012–19
9. Shi W, Zhang C, Ning Z et al: Long non-coding RNA LINC00346 promotes pancreatic cancer growth and gemcitabine resistance by sponging miR-188-3p to derepress BRD4 expression. *J Exp Clin Cancer Res*, 2019; 38(1): 60
10. Meng F, Zhang S, Song R et al: NCAPG2 overexpression promotes hepatocellular carcinoma proliferation and metastasis through activating the STAT3 and NF- κ B/miR-188-3p pathways. *EBioMedicine*, 2019; 44: 237–49
11. Zhang XF, Yang Y, Yang XY, Tong Q: MiR-188-3p up-regulation results in the inhibition of macrophage proinflammatory activities and atherosclerosis in ApoE-deficient mice. *Thromb Res*, 2018; 171: 55–61
12. Engel FB, Hsieh PC, Lee RT, Keating MT: FGF1/p38 MAP kinase inhibitor therapy induces cardiomyocyte mitosis, reduces scarring, and rescues function after myocardial infarction. *Proc Natl Acad Sci USA*, 2006; 103(42): 15546–51
13. Zhang L, Cheng H, Yue Y et al: TUG1 knockdown ameliorates atherosclerosis via up-regulating the expression of miR-133a target gene FGF1. *Cardiovasc Pathol*, 2018; 33: 6–15

14. Wang YS, Wang HY, Liao YC et al: MicroRNA-195 regulates vascular smooth muscle cell phenotype and prevents neointimal formation. *Cardiovasc Res*, 2012; 95(4): 517–26
15. Brogi E, Winkles JA, Underwood R et al: Distinct patterns of expression of fibroblast growth factors and their receptors in human atheroma and non-atherosclerotic arteries. Association of acidic FGF with plaque microvessels and macrophages. *J Clin Invest*, 1993; 92(5): 2408–18
16. Xu CX, Xu L, Peng FZ et al: MiR-647 promotes proliferation and migration of ox-LDL-treated vascular smooth muscle cells through regulating PTEN/PI3K/AKT pathway. *Eur Rev Med Pharmacol Sci*, 2019; 23(16): 7110–19
17. Chen LY, Xia XD, Zhao ZW et al: MicroRNA-377 inhibits atherosclerosis by regulating triglyceride metabolism through the DNA methyltransferase 1 in apolipoprotein E-knockout mice. *Circ J*, 2018; 82(11): 2861–71
18. Pei J, Zhang J, Yang X et al: TMED3 promotes cell proliferation and motility in breast cancer and is negatively modulated by miR-188-3p. *Cancer Cell Int*, 2019; 19: 75
19. Wang L, Zheng M, Wu S, Niu Z: MicroRNA-188-3p is involved in sevoflurane anesthesia-induced neuroapoptosis by targeting MDM2. *Mol Med Rep*, 2018; 17(3): 4229–4236.
20. Ananyeva NM, Tjurmin AV, Berliner JA et al: Oxidized LDL mediates the release of fibroblast growth factor-1. *Arterioscler Thromb Vasc Biol*, 1997; 17(3): 445–53
21. Ghiselli G, Chen J, Kao M et al: Ethanol inhibits fibroblast growth factor-induced proliferation of aortic smooth muscle cells. *Arterioscler Thromb Vasc Biol*, 2003; 23(10): 1808–13
22. Cai T, Cui X, Zhang K et al: LncRNA TNK2-AS1 regulated ox-LDL-stimulated HASMC proliferation and migration via modulating VEGFA and FGF1 expression by sponging miR-150-5p. *J Cell Mol Med*, 2019; 23(11): 7289–98
23. Zakrzewska M, Opalinski L, Haugsten EM et al: Crosstalk between p38 and Erk 1/2 in downregulation of FGF1-induced signaling. *Int J Mol Sci*, 2019; 20(8): E1826
24. Wang D, Jin M, Zhao X et al: FGF1^{AHBS} ameliorates chronic kidney disease via PI3K/AKT mediated suppression of oxidative stress and inflammation. *Cell Death Dis*, 2019; 10(6): 464